CERN – EUROPEAN ORGANIZATION FOR NUCLEAR RESEARCH

CLIC – Note – 1197

SINGLE CYLINDER CAVITY BASED RF CAVITIES FOR KLYSTRON-BASED COMPACT LINEAR COLLIDER

P. Wang and A. Grudiev

CERN, Geneva, Switzerland

Abstract

The proposed pulse compression system for the klystron-based Compact Linear Collider (CLIC) is based on individual cavities. The essential requisites for this system encompass are easy fabrication, optimal RF performance, and cost-effectiveness. We have identified two novel RF cavity types which can be used as correction cavities for klystron-based CLIC pulse compression system, characterized by their compactness, advantageous large pass band or low surface field, and ease of fabrication. Both RF cavity types adopt a cylindrical resonant cavity with T E223 mode, employing four coupling holes to induce T E223 modes with dual polarizations. Power flow direction is facilitated by a U-shaped waveguide and a 3-dB Hybrid in two layouts. A comprehensive discussion on the principles underlying these RF cavity types is provided. Additionally, we elucidate the RF designs of the individual cavities for principle demonstration. Furthermore, these two RF cavity types can be readily adapted to other operational frequencies, such as C-band and S-band.

Geneva, Switzerland
May 2024

Single cylinder cavity based RF cavities for klystron-based Compact Linear Collider

Ping Wang and Alexej Grudiev[*]
CERN, Geneva, Swtizerland

Abstract
The proposed pulse compression system for the klystron-based Compact Linear Collider (CLIC) is based on individual cavities. The essential requisites for this system encompass are easy fabrication, optimal RF performance, and cost-effectiveness. We have identified two novel RF cavity types which can be used as correction cavities for klystron-based CLIC pulse compression system, characterized by their compactness, advantageous large pass band or low surface field, and ease of fabrication. Both RF cavity types adopt a cylindrical resonant cavity with TE_{223} mode, employing four coupling holes to induce TE_{223} modes with dual polarizations. Power flow direction is facilitated by a U-shaped waveguide and a 3-dB Hybrid in two layouts. A comprehensive discussion on the principles underlying these RF cavity types is provided. Additionally, we elucidate the RF designs of the individual cavities for principle demonstration. Furthermore, these two RF cavity types can be readily adapted to other operational frequencies, such as C-band and S-band.

Keywords
Correction cavity; RF Pulse compressor; CLIC.

1 Introduction

Klystron-based electron-positron colliders have a rich historical background, exemplified by the SLAC Linear Collider (SLC), VLEPP project, the Japan Linear Collider (JLC), and the Next Linear Collider (NLC) [1–4]. In these colliders, the implementation of a RF pulse compression system is essential to increase the RF peak power, thus reducing the cost of the RF system. For instance, the SLED pulse compressor was utilized for SLC, the Barrel Open Cavity (BOC) based VLEEP Power Multiplier (VPM) for VLEPP, a cavity chain based SLED pulse compressor for JLC, and a long delay line based SLED-II pulse compressor for NLC [5–8].

The Compact Linear Collider(CLIC), featuring two-beam scheme, was proposed for high-energy applications at the TeV scale, such as 1.5 TeV and 3 TeV. In this scheme, a high current driven beam traverses the Power Extraction Structures, generating RF power for the accelerating structures, thereby eliminating the need for klystrons in the main linac. Consequently, the two-beam scheme offers the advantage of cost-effectiveness. However, at low energies, such as 380 GeV, the drive beam remains the same as that used for higher energies, resulting in a relatively increase in the cost of RF power for each accelerating structure. Due to this factor, the klystron-based CLIC emerges as a viable alternative, akin to other aforementioned colliders.

To maximize the number of electrons, multi-bunch acceleration is implemented in JLC NLC and CLIC. JLC proposed a SLED-type pulse compressor employing two coupled cavity chains and a 3-dB hybrid, while NLC proposed the SLED-II pulse compressor utilizing two long delay lines and a 3-dB hybrid [7, 8]. In frequency domain, SLED-II pulse compressor exhibits numerous RF peaks in its spectrum, whereas the JLC pulse compressor displays only three RF peaks in its spectrum. In contrast,

[*]ping.wang@cern.ch.

the klystron-based CLIC employs a pulse compression system that lies between the two aforementioned RF pulse compressors, concerning the number of RF peaks. This pulse compression system comprises a storage cavity with a large unloaded quality factor and several correction cavities with relatively low unloaded quality factors, where the number of the RF peaks corresponds to the number of the cavities. The original concept of this pulse compressor dates back to 1990, subsequently undergoing detailed investigation at CERN [9].

Three correction cavity chains were investigated, incorporating cylinder cavities, mini BOCs, and corrugated cavities [10]. The first RF Rotator, utilizing a 3 dB hybrid and a mode convertor, was specifically tailored for the corrugated cavity [10]. SLAC developed another RF Rotator, referred to as the dual-mode polarizer, featuring a simple geometry [11]. While serving the same purpose as corrugated cavity RF Rotator, its straigntforward design facilitates fabrication. We engineered and manufactured the first correction cavity chain employing four RF Rotators and eight spherical cavities with mode TE_{112} [12, 13]. A similar correction cavity chain was devised and constructed for the Tsinghua X-band high-power test stand [14].

For the klystron-based CLIC, the current correction cavity chain at CERN proves unsuitable. The pulse compression system is designed for a pulse length of 250 ns, corresponding to an RF peak separation of 5 MHz. However, the CLIC-K structure, designed for klystron-based CLIC, necessitates a input pulse length of 350 ns, requiring a smaller RF peak separation [15]. Additionally, the optimal number of correction cavities was investigated, considering the pulse shape and RF loss. It was determined that four cavities, rather than eight, would the most effective. Therefore, the correction cavity must be updated to align with the requirements of the klystron-based CLIC.

The investigation into the next correction cavity chain introduced the concept of a bowl cavity [16]. This cavity's design closely resembles that of the spherical pulse compressor, which relies on an RF Rotator. In the bowl cavity, two polarized modes are excited. Currently, the bowl cavity serves as the baseline for the correction cavity. However, the exploration of new concepts and RF designs is encouraged, particularly if they offer cost benefits. With a anticipated about 10000 correction cavities in the main linac, any enhancement to their design is valuable.

To ensure a cost-effective correction cavity, it is imperative to maintain a simple geometry. Such simplicity facilitates all procedures including machining, metrology, and integration. Among resonant cavity geometries, the Cylinder stands out as the simplest. Notably, the majority of SLED pulse compressors empoly two identical cylinder cavities [5]. Furthermore, given that both BOC pulse compressor and RF rotator based pulse compressors operate effectively with just one cavity, it serve as a fundamental requirement. Additionally, the design of the waveguide directing RF power flow should prioritize simplicity [17–22]. In line with these criteria, two novel RF cavity types, based on cylinder cavities, are proposed for correction cavities of the klystron-based CLIC. This paper will elaborate on the principles and RF designs of these RF cavity types, highlighting their potential scalability to other frequencis for diverse applications.

2 Principles of the two new RF cavity types

From a mechanical design perspective, SLED pulse compressors typically consist of two identical cavities, whereas the BOC and RF rotator based RF pulse compressors can operate effectively with one resonant cavity. However, from an RF design standpoint, they share similarities. In the case of a single-cavity setup, two poliarzed modes perform the same function as the two resonant cavities in the traditional SLED pulse compressors. The RF pulse compressor's behavior can be elucidated by considering the RF parameters of the resonant cavity and the S-parameters of associated waveguide network (a 3-dB hybrid for SLED pule compressors, and waveguide surrounding the cavity for BOC pulse compressors, and the RF rotator for RF rotator based RF pulse compressors). The characteristics of the resonant cavity can be

described as:

$$\Gamma = \frac{(\beta - 1) - jQ_0\xi}{(\beta + 1) + jQ_0\xi}, \tag{1}$$

where, β represents the coupling factor of the resonant cavity, Q_0 denotes the unloaded quality factor and ξ is defined as follows: $\xi = f/f_0 - f_0/f$. Here, f_0 represents the resonant frequency of the resonant cavity. The waveguide networks mentioned earlier can be viewed as a four-port device, with two ports designated as input and output, while the other two ports are linked to the cavity. These waveguide networks can be described by a 16-item matrix:

$$M_{wg} = \begin{bmatrix} s_{11} & s_{12} & s_{13} & s_{14} \\ s_{21} & s_{22} & s_{23} & s_{24} \\ s_{31} & s_{32} & s_{33} & s_{34} \\ s_{41} & s_{42} & s_{43} & s_{44} \end{bmatrix} \tag{2}$$

The RF pulse compressor model can be considered akin to the frequency domain model employed for RF rotator based RF pulse compressors [23]. By incorporating the cavity or cavities onto the waveguide networks, a two-port device with input and output ports is obtained. The matrix representation of the two-port device is as follows:

$$M_{PC} = \begin{bmatrix} s_{11}^{PC} & s_{12}^{PC} \\ s_{21}^{PC} & s_{22}^{PC} \end{bmatrix}, \tag{3}$$

$$s_{11}^{PC} = s_{11} + \frac{s_{14}s_{41}\left(\frac{1}{\Gamma_1} - s_{33}\right) + s_{13}s_{31}\left(\frac{1}{\Gamma_2} - s_{44}\right) + s_{14}s_{43}s_{31} + s_{13}s_{34}s_{41}}{\left(\frac{1}{\Gamma_2} - s_{44}\right)\left(\frac{1}{\Gamma_1} - s_{33}\right) - s_{34}s_{43}}, \tag{4}$$

$$s_{12}^{PC} = s_{12} + \frac{s_{14}s_{42}\left(\frac{1}{\Gamma_1} - s_{33}\right) + s_{13}s_{32}\left(\frac{1}{\Gamma_2} - s_{44}\right) + s_{14}s_{43}s_{32} + s_{13}s_{34}s_{42}}{\left(\frac{1}{\Gamma_2} - s_{44}\right)\left(\frac{1}{\Gamma_1} - s_{33}\right) - s_{34}s_{43}}, \tag{5}$$

$$s_{21}^{PC} = s_{21} + \frac{s_{24}s_{41}\left(\frac{1}{\Gamma_1} - s_{33}\right) + s_{23}s_{31}\left(\frac{1}{\Gamma_2} - s_{44}\right) + s_{24}s_{43}s_{31} + s_{23}s_{34}s_{41}}{\left(\frac{1}{\Gamma_2} - s_{44}\right)\left(\frac{1}{\Gamma_1} - s_{33}\right) - s_{34}s_{43}}, \tag{6}$$

$$s_{22}^{PC} = s_{22} + \frac{s_{24}s_{42}\left(\frac{1}{\Gamma_1} - s_{33}\right) + s_{23}s_{32}\left(\frac{1}{\Gamma_2} - s_{44}\right) + s_{24}s_{43}s_{32} + s_{23}s_{34}s_{42}}{\left(\frac{1}{\Gamma_2} - s_{44}\right)\left(\frac{1}{\Gamma_1} - s_{33}\right) - s_{34}s_{43}}, \tag{7}$$

where, Γ_1 and Γ_2 represent the reflections of the two modes in a single cavity or the reflections of the two resonant cavities. In ideal scenario, the matrix of the waveguide networks takes the following form:

$$M_{wg} = \frac{1}{\sqrt{2}} \begin{bmatrix} 0 & 0 & 1 & i \\ 0 & 0 & i & 1 \\ 1 & i & 0 & 0 \\ i & 1 & 0 & 0 \end{bmatrix}, \tag{8}$$

The s-parameters of the RF pulse compressors under ideal conditions are as follows:

$$M_{PC} = \begin{bmatrix} \frac{1}{2}(\Gamma_1 - \Gamma_2)) & \frac{i}{2}(\Gamma_1 + \Gamma_2)) \\ \frac{i}{2}(\Gamma_1 + \Gamma_2)) & \frac{1}{2}(\Gamma_2 - \Gamma_1)) \end{bmatrix}, \tag{9}$$

The frequency response in the frequency domain for the RF pulse compressor results from the combination of the reflections from two polarized modes within one cavity or the reflections from two resonant cavities. Currently, three schemes are utlilized for RF pulse compressors: the 3-dB hybrid with two identical cavities, the RF rotator with a resonant cavities featuring polarized modes, and the Barrel Open Cavity with surrounding waveguide. The key characteristics of the single cavity based RF pulse compressor can be summarized as follows: the presence of two polarized modes within the cavity is a fundamental requirement. In the case of BOC pulse compressor, the two polarized modes are excited by different coupling holes, while in the RF rataor based RF pulse compressor, they are excited by the two TE_{11} modes within the circular waveguide of the RF rotator.

This paper proposes a cylinder cavity featuring polarized TE_{223} modes, illustrated in the Fig 1. The cavity can be effectively simulated by utilizing a quarter of the cylinder with the E face and H face serving as the symmetric planes. The unloaded quality factor of the cavity is 57000. The mode separation from adjacent modes is 45 MHz. To excite the polarized modes, two RF networks are empolyed: a U-shape waveguide (USW) and a compact 3-dB hybrid. In both cases, four coupling holes facilitate the coupling process, albeit with differing underling principles.

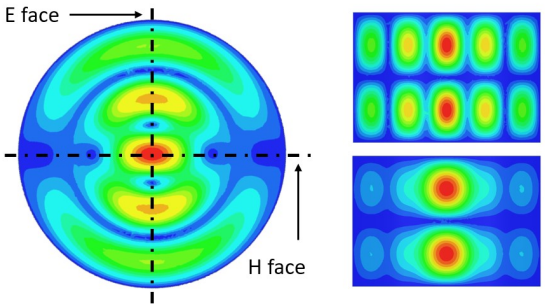

Figure 1: TE_{223} mode of the cylinder cavity

The principle of the USW based layout resembles that of the BOC pulse compressor. The USW based layout, along with its main parameters is depicted in the Fig 2. RF power traverses the USW, exciting two polarized modes within the cavity. The parameter dr denotes the distance bteween the coupling holes, which must align with the width of the waveguide for both polarized modes. The the matched case, the RF parameters of the two polarized modes are identical, and their phases exhibit a 90-degree difference. The field establishment procedure is illustrated in the Fig 3. At the two coupling holes(CP), the RF power experiences a phase different of 90 degrees. The field generated in the cavity by each coupling hole is split into two parts with opposite directions. As the field from CP2 reaches CP1, it becomes out of phase with the field from CP1. Conversely, when the field from CP1 reaches CP2, it alighs in phase with the field from CP2. Consequently, this procedure ensures consistent power flow directions both within the waveguide and cavity. Likewise, when RF power exits the cavity, the power flow mirrors that with the cavity, owing to the same underlying principles discussed earlier.

The layout based on the 3-dB bybrid employs a novel principle that has never been previously utilized. Typically, the 3-dB hybrid operates in conjunction with two resonant cavities. The 3-dB hybrid based layout, along with its main parameters, is illustrated in the Fig 4. RF port-1 and port-2 are linked to a 3-dB hybrid, resulting in the input RF power with a 90-degree phase difference. RF power entering RF port-1 and port-2 excites the polarized modes, indicated by the red and green arrows respectively. For

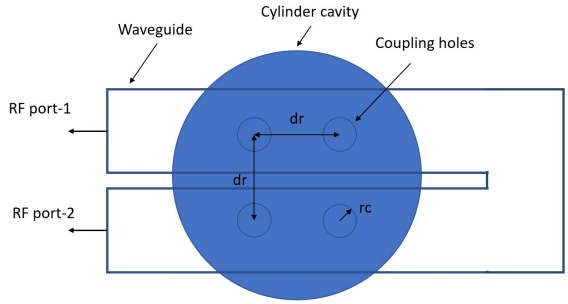

Figure 2: USW based layout with main parameters

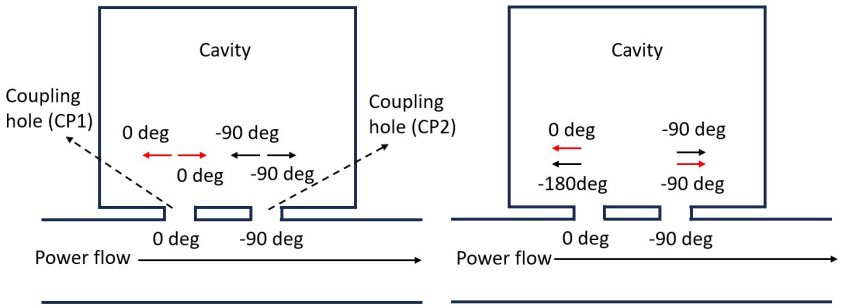

Figure 3: Field establishment of the USW based layout

input power from RF port-1, only the green coupling holes are utilized for coupling, while for the input power from RF port-2, the other two red coupling holes are employed. The resulting excited modes are orthogonal.

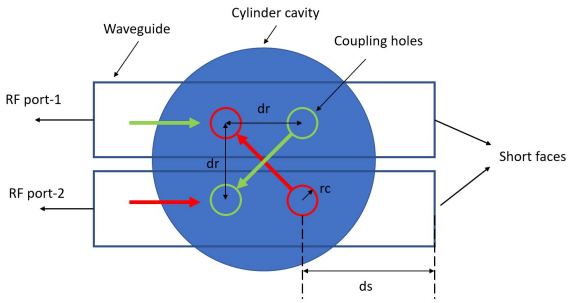

Figure 4: 3-dB hybrid based scenario with main parameters

3 RF design of the USW based layout

The RF design of the USW based layout comprises a cylinder cavity, four coupling holes and a U-shape waveguide, illustrated in the Fig 5. Four small pins on the cylinder cavity are employed to slightly adjust the frequency of one polarization. The RF design features a straightforward geometry that facilitates the

fabrication procedure.

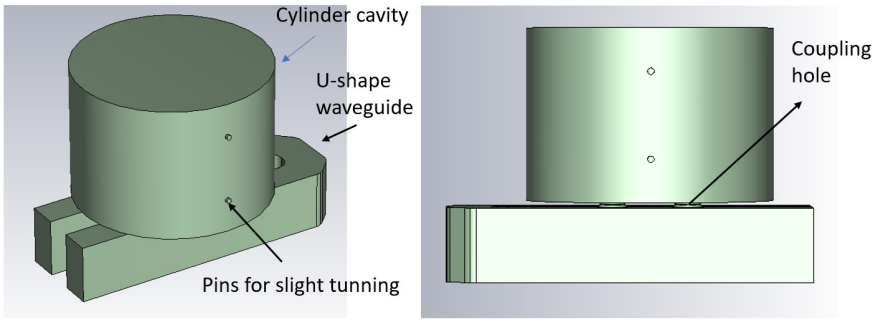

Figure 5: RF design of the USW based scenario

The RF design process commences with the simplified model depicted in the Fig 6. A half of the cylinder cavity, with master and slave boundaries, is employed to calculate the RF parameters. Both ports of the waveguide are terminated by Perfect Matching Layers (PML). The resonant cavity's frequency is adjusted by altering the cavity's height, while coupling is fine-tuned by varying the radius of the coupling holes. To ensure identical coupling factors for the two polarized modes, the spacing between the coupling holes is adjusted. The RF design and s-parameters of the USW are shown in the Fig 7 and 8. The pass band, defined by the reflection below -30 dB, is 76 MHz. Compared to the RF rotator, the USW has a simpler geometry, making it is easier to fabricate.

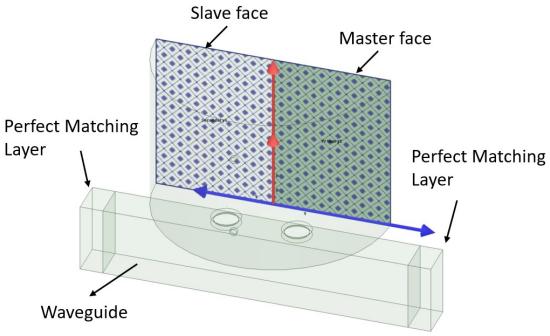

Figure 6: Simplified RF model of the USW based layout

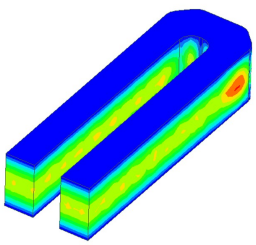

Figure 7: RF design of the USW

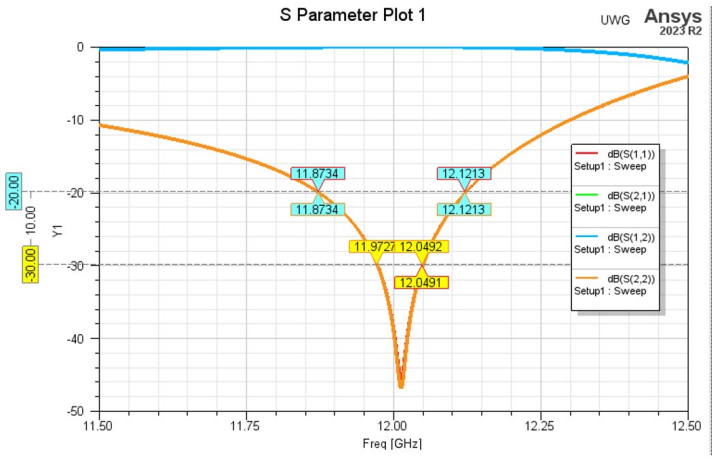

Figure 8: S-parameters of the USW

Upon finalizing the USW and optimizing the cavity with coupling hole, the RF design is completed. The field distribution of the RF pulse compressor is shown in the Fig 9. Essentially, the field inside the cavity exhibits a rotating feature, akin to that of the BOC pulse compressor and RF rotator based RF pulse compressor. The final s-parameters of the USW based RF cavity type are shown in the Fig 10. The reflection of the full RF design has been optimized to a level below -25 dB, deemed sufficient for the correction cavity. Given that the frequencies of the correction cavities are more 3 MHz away from the normal frequency of 11.994 GHz. The frequency of the current RF design stands at 11.9935 GHz. This frequency can be easily adjusted during the design phase of the final correction cavity chain. The RF parameters and surface fields are calculated based on the full RF model, which will be elaborated upon in the subsequent discussions.

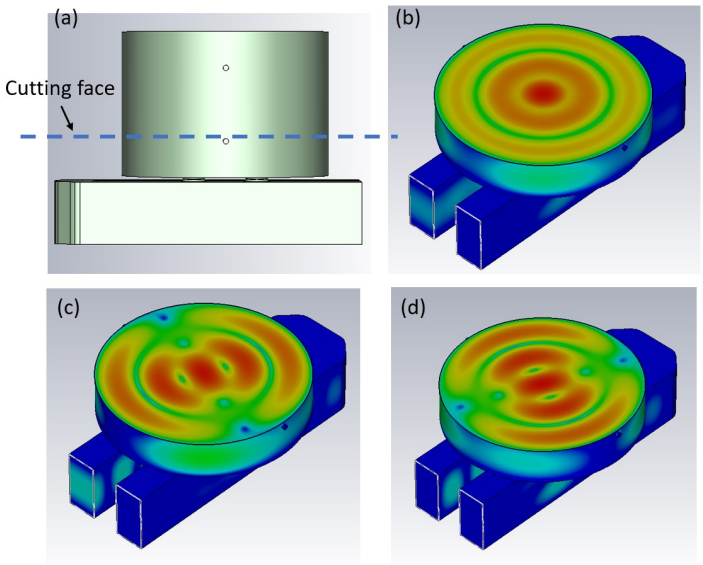

Figure 9: Field distribution of the USW based RF cavity type. (a) position of the cutting face (b) complex electric field (c) electric field with phase of 0 degree (d) electric field with phase of 90 degree

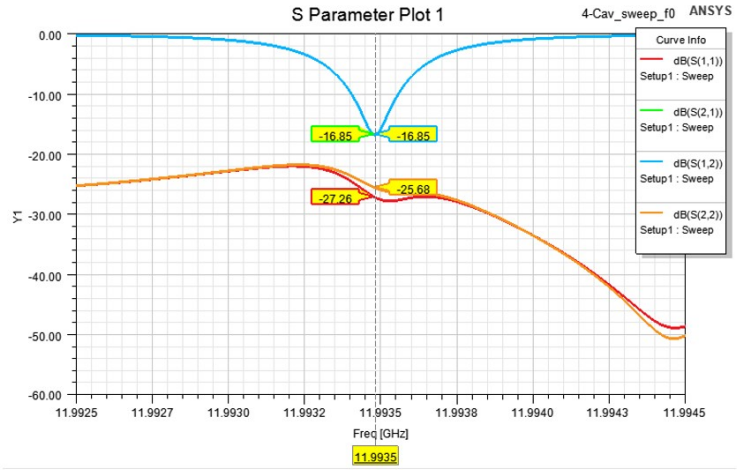

Figure 10: S-parameters of the USW based RF cavity type

4 RF design of the 3-dB hybrid based layout

The RF design of the 3-dB based RF cavity type is shown in the Fig 11, featuring a cylinder cavity, a compact 3-dB hybrid, and 4 coupling holes. Notably, the 3-dB hybrid utilized in this design is identical to the one employed in the new RF module for Klystron-based CLIC [24]. The RF design process initiates with a simplified RF model based on a half cylinder cavity as shown in Fig 12. The input port is terminated by a PML, while the symmetric face serves as either E face or H face for calculating the RF parameters of the two polarized modes. Adjustments to the radius facilitate coupling tuning, while fine-tuning the distance between the coupling holes and the position of the short face ensures uniform RF parameters for the two polarized modes.

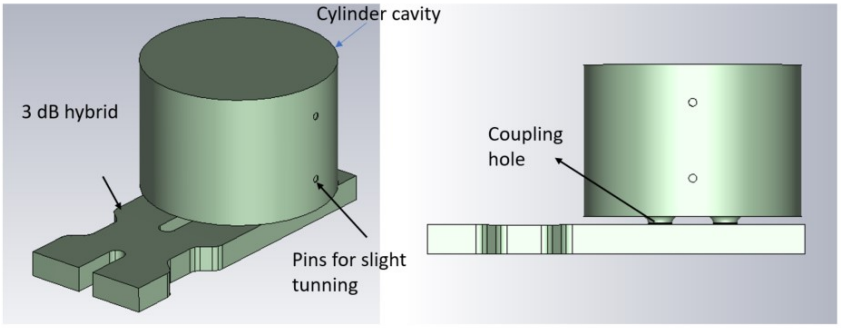

Figure 11: RF design of the 3-dB hybrid based RF cavity type

The RF design and the s-parameters are shown in the Figs 13 and 14. The pass band of the 3-dB hybrid, defined by the reflection below -30 dB, is more than 300 MHz.

After optimizing the cavity and integrating the 3-dB hybrid, the final RF design of the 3-dB hybrid based RF cavity type is obtained. The field distributions of the RF cavity type are shown in the Fig 15. The features of the field distributions mirror those of the USW based RF cavity type. The s-parameters of the full RF design are shown in the Fig 16. The current RF design operates at a frequency of 11.995 GHz,

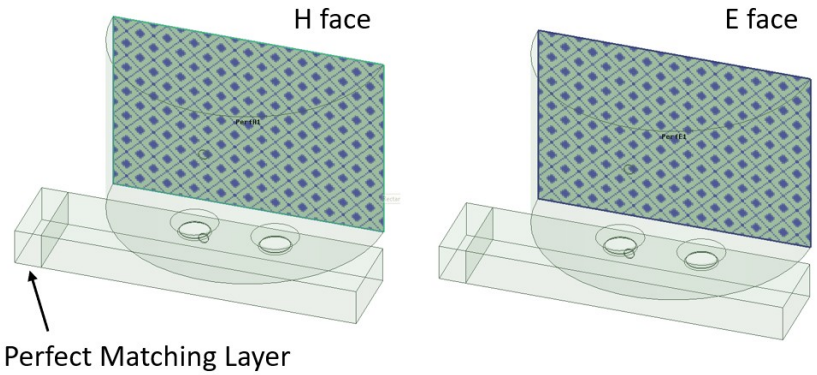

Figure 12: Simplified RF model for the 3-dB hybrid based RF cavity type

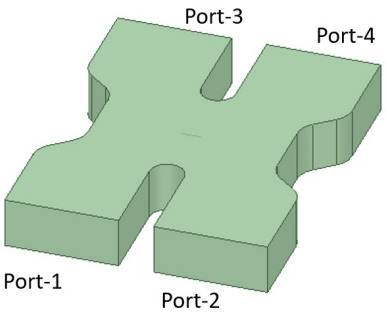

Figure 13: RF design of the compact 3-dB hybrid

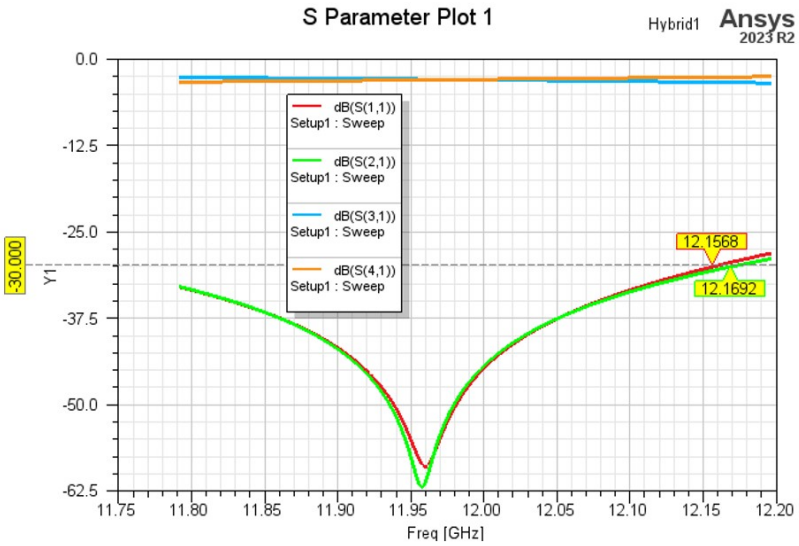

Figure 14: S-parameters of the compact 3-dB hybrid

which is very close to the normal frequency of the klystron-based CLIC. Furthermore, the frequency can be easily modified as needed.

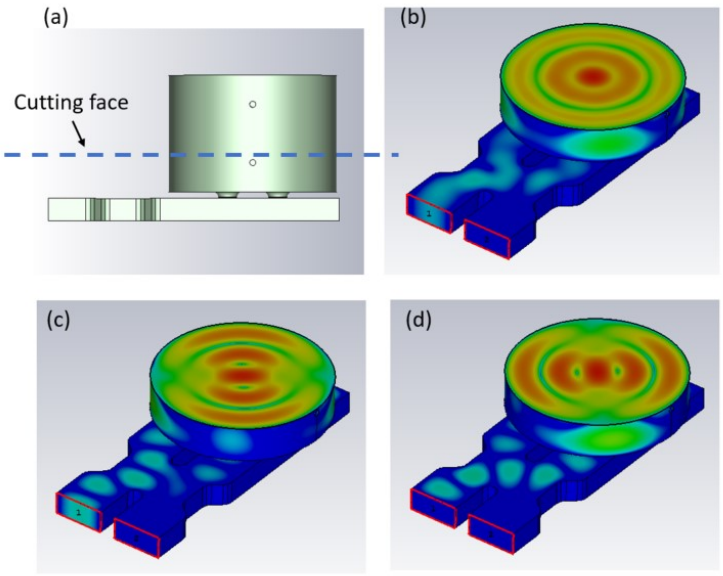

Figure 15: Field distribution of the 3-dB hybrid based RF cavity type. (a) position of the cutting face (b) complex electric field (c) electric field with phase of 0 degree (d) electric field with phase of 90 degree

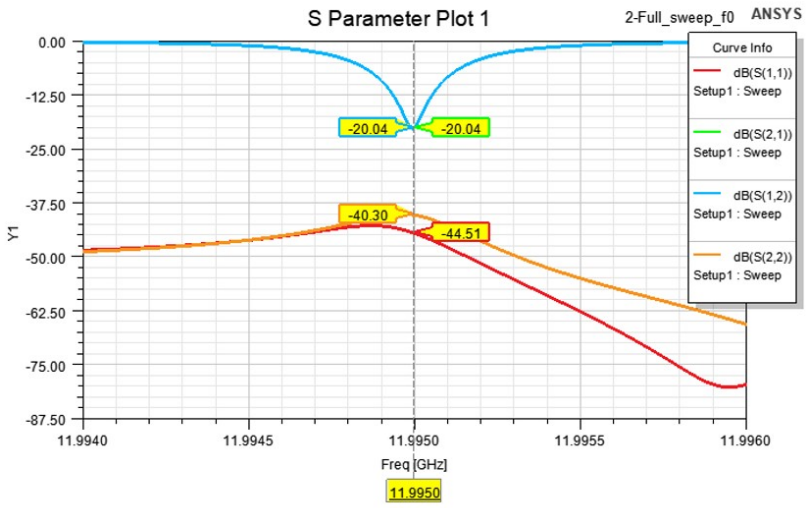

Figure 16: S-parameters of the 3-dB hybrid based RF cavity type

5 Comparison of the RF cavity types

The fundamental requirements of the correction cavity for klystron-based CLIC are compact size and ease of fabrication. The current bowl cavity based RF cavity type serves as the baseline, providing a reference point for comparison. The RF parameters and surface fields are summarized in the table 1.

Surface fields are calculated by using a frequency of $f_0 + 3$ MHz, where the f_0 represents the resonant frequency. The frequency offset of 3 MHz accounts for the pulse length for the klystron-based CLIC. Pass bands are defined by the reflections below -20 dB and -30 dB. The couplings for the three RF pulse compressors are optimized to match the storage cavity in the klystron-based CLIC.

As the baseline, the bowl cavity based cavity type offers the advantage of a large unloaded quality factor. However, this advantage comes at cost of a large volume. Another benefit is that the principle of the bowl cavity has been successfully demonstrated, making it a relatively proven technique. In contrast, the other two RF cavity types feature smaller unloaded quality factors but also also smaller volumes. Both of these RF cavity types offer larger pass bands, particularly the 3-dB hybrid based one. The USW based cavity type boasts the smallest surface electric field, which is advantageous for reducing breakdown rates. Moreover, the geometries of the two new RF cavity types are much simpler than that of the the bowl cavity based one. Consequently, the fabrication procedure of the two new RF cavity types is expected to be easier, resulting in cost-effectiveness.

Table 1: Comparison of the 3 RF cavity types for correction cavities

Heading	**Bowl**	**USW**	**Hybrid**
Cavity volume [mm^3]	5.8e5	2.46e5	2.46e5
Unloaded quality factor	7.5e4	5.3e4	5.0e4
Coupling factor	1.9	1.3	1.2
band width [MHz@-30dB]	70	80	130
band width [MHz@-20dB]	260	250	>300
Emax [MV/m]	40.6	25.5	62.8
Hmax [kA/m]	86.3	105.2	159

The relationship between the unloaded quality factor and the frequency of a normal temperature resonant cavity is given by: $Q_0 \propto 1/f$. Take the S-band case as a example, a cavity operating at the S-band frequency of 2998 MHz typically exhibits an unloaded quality factor of 100,000, a common value for the S-band RF pulse compressors.

6 Conclusion

Two new RF cavity types have been investigated for the correction cavities of the klystron-based CLIC. They utilize a simple cylinder cavity with a mode of TE_{223}. These designs are characterized by their compactness and ease for fabrication. The principles and RF designs of these two RF cavity types are discussed in detail. Furthermore, these principle and RF designs can be applied to other frequencies as well.

Bibliography

[1] John T Seeman. The stanford linear collider. *Annual Review of Nuclear and Particle Science*, 41(1):389–428, 1991.

[2] VE Balakin, VA Sidorov, and AN Skrinsky. The vlepp project status report. *preprint INP-81-129, Novosibirsk*, 1981.

[3] SEISHI Takeda. Japan linear collider (jlc). *Part. Accel.*, 30:143–152, 1990.

[4] T Raubenheimer, C Adolphsen, D Burke, P Chen, S Ecklund, J Irwin, G Loew, T Markiewicz, R Miller, E Paterson, et al. Parameters of the slac next linear collider. In *proceedings particle accelerator conference*, volume 2, pages 698–700. IEEE, 1995.

[5] ZD Farkas, HA Hogg, GA Loew, and Pj B Wilson. Sled: A method of doubling slac's energy. In *Proc. Of 9th Int. Conf. On High Energy Accelerators, SLAC*, page 576, 1974.

[6] VE Balakin and IV Syrachev. Status of vlepp rf power multiplier (vpm). *Proc. of EPAC92*, pages 1173–1175, 1992.

[7] H Matsumoto, Su Su Win, KEK Shigeru Takeda, Y Takasu, and M Yoshida. Kek c-band rf system r&d status for linear collider. In *Proc. of 28th LINAC Meeting*, 2003.

[8] Sami G Tantawi, Christopher D Nantista, Valery A Dolgashev, Chris Pearson, Janice Nelson, Keith Jobe, Jose Chan, Karen Fant, Josef Frisch, and Dennis Atkinson. High-power multimode x-band rf pulse compression system for future linear colliders. *Physical Review Special Topics-Accelerators and Beams*, 8(4):042002, 2005.

[9] S Yu Kazakov. Pulse shape correction for rf pulse compression system. *Spectrum*, 5(7):9, 1992.

[10] I. Syratchev. Table-top sledii pulse compressor. HG2013, 3-6 June, 2013, ICTP Trieste, Italy.

[11] Juwen W. Wang, Sami G. Tantawi, Chen Xu, Matt Franzi, Patrick Krejcik, Gordon Bowden, Shantha Condamoor, Yuantao Ding, Valery Dolgashev, John Eichner, Andrew Haase, James R. Lewandowski, and Liling Xiao. Development for a supercompact x-band pulse compression system and its application at slac. *Phys. Rev. Accel. Beams*, 20:110401, Nov 2017.

[12] Ping Wang, Hao Zha, Igor Syratchev, Jiaru Shi, and Huaibi Chen. rf design of a pulse compressor with correction cavity chain for klystron-based compact linear collider. *Phys. Rev. Accel. Beams*, 20:112001, Nov 2017.

[13] Yuliang Jiang, Hao Zha, Ping Wang, Jiaru Shi, Huaibi Chen, William L Millar, and Igor Syratchev. Demonstration of a cavity-based pulse compression system for pulse shape correction. *Phys. Rev. Accel. Beams*, 22:082001, Aug 2019.

[14] Xiancai Lin, Hao Zha, Jiaru Shi, Yuliang Jiang, Fangjun Hu, Weihang Gu, Qiang Gao, and Huaibi Chen. x-band two-stage rf pulse compression system with correction cavity chain. *Phys. Rev. Accel. Beams*, 25:120401, Dec 2022.

[15] Jinchi Cai and Igor Syratchev. The design update of the X-band RF pulse compressor with Correction Cavities for the CLIC 380 GeV klystron based accelerator. Technical report, CERN, Geneva, 2020.

[16] Xiaowei Wu and Alexej Grudiev. Novel open cavity design for rotating mode rf pulse compressors. *Phys. Rev. Accel. Beams*, 24:112001, Nov 2021.

[17] P. Brown and I. Syratchev. 3 ghz barrel open cavity (boc) rf pulse compressor for ctf3. In *2004 IEEE MTT-S International Microwave Symposium Digest (IEEE Cat. No.04CH37535)*, volume 2, pages 1009–1012 Vol.2, 2004.

[18] R Zennaro, M Bopp, A Citterio, R Reiser, T Stapf, et al. C-band rf pulse compressor for swissfel. *Proc. IPAC*, pages 2827–2829, 2013.

[19] Guan Shu, Feng-Li Zhao, and Xiang He. Rf study of a c-band barrel open cavity pulse compressor. *Chinese Physics C*, 39(5):057005, 2015.

[20] Yuliang Jiang, Hao Zha, Jiaru Shi, Maomao Peng, Xiancai Lin, and Huaibi Chen. A compact x-band microwave pulse compressor using a corrugated cylindrical cavity. *IEEE Transactions on Microwave Theory and Techniques*, 69(3):1586–1593, 2021.

[21] Zongbin Li, Wencheng Fang, Qiang Gu, and Zhentang Zhao. Rf design of a c-band compact spherical rf pulse compressor for sxfel. *Nuclear Instruments and Methods in Physics Research Section A: Accelerators, Spectrometers, Detectors and Associated Equipment*, 863:7–14, 2017.

[22] Jie Lei, Xiang He, Mi Hou, Guan Shu, Guo-Xi Pei, Xiao-Ping Li, and Hui Wang. Rf design of an s-band spherical cavity pulse compressor. *Radiation Detection Technology and Methods*, 1(2):16, 2017.

[23] Ping Wang, Jiaru Shi, Hao Zha, Dezhi Cao, Maomao Peng, Zening Liu, Cheng Cheng, and Huaibi Chen. Development of an s-band spherical pulse compressor. *Nuclear Instruments and Methods in Physics Research Section A: Accelerators, Spectrometers, Detectors and Associated Equipment*,

901:84–91, 2018.

[24] Ping Wang, Matthew John Capstick, Nuria Catalan Lasheras, Steffen Doebert, Alexej Grudiev, Carlo Rossi, Pedro Morales Sanchez, Igor Syratchev, and Xiaowei Wu. Design of the RF waveguide network for the klystron-based CLIC main linac RF Module. Technical report, CERN, Geneva, 2024.